Role of $CoBr_2$ on the Structural, Optical and Magnetic Properties of Polyvinyl Alcohol Films

I. S. Elashmawi,[1] E. M. Abdelrazek[2]

[1]*Spectroscopy Department, Physics Division, National Research Centre, Dokki, Giza, Egypt*
[2]*Physics Department, Faculty of Science, Mansoura University, 35516, Mansoura, Egypt*

Received 9 March 2008; accepted 8 December 2008
DOI 10.1002/app.29859
Published online 26 October 2009 in Wiley InterScience (www.interscience.wiley.com).

ABSTRACT: Polyvinyl alcohol (PVA) films filled with different concentrations of $CoBr_2$ were prepared using the casting method. These films were characterized by FTIR, UV–visible, XRD, and ESR techniques. FTIR spectra were used to clarify the structural variations due to the filling level from $CoBr_2$. The observed bands at 3484, 1733, and 1640 cm^{-1} were assigned to O—H, C=O, and C=C stretching vibrations, respectively. UV–visible spectra shows the absorption band at 280 nm which is assigned to $\pi \rightarrow \pi^*$ transition. This indicates the presence of unsaturated bonds in tail to head of PVA. Optical energy gap decreased with increasing the concentration of $CoBr_2$. X-ray diffraction scans show some decrease in the degree of crystallinity in the filled films which reveals an increase in amorphous phase of PVA due to the interaction between Co^{+2} and polymeric matrix causing a molecular rearrangement within the amorphous phase of PVA. The observed complex ESR spectrum due to hyperfine interactions confirms the role of free radicals. Spectroscopic and magnetic properties of PVA/$CoBr_2$ composite films were investigated and compared with those of PVA alone. The results show that the change of the structure due to the interaction of filler with the polymer. J Appl Polym Sci 115: 2691–2696, 2010

Key words: polyvinyl alcohol; FTIR; UV–visible; X-ray; ESR

INTRODUCTION

PVA is characterized by its several interesting properties which make it as a useful material in a wide verity of applications.[1,2] PVA has different internal structure which may amorphous or semicrystalline. The semicrystalline structure of PVA showed an important feature rather than of amorphous one. This is may be because semicrystalline PVA leads to formation of both crystalline and amorphous regions.

PVA is considered as a poor electric conductor and it can become semiconductive upon doping with some dopant. Conducting nature of doped PVA is reported to be due to interactions between polymer chains and dopant via hydrogen bonding with hydroxyl-groups as well as the complex formation. PVA is also recognized as one of the very few vinyl polymers soluble in water with a high transparency and a good flexibility.

Recently, PVA films are doped with multiple valance metal ions and showed that a strong dependence of donor–acceptor mechanism between the metal ion and the polymer matrix. Several authors[3–8] have studied the optical, structural, and other properties of PVA with different dopant like, $CuCl_2$, $AgNO_3$, $MnCl_2$, $BaCl_2$, $MgBr_2$, and $FeCl_3$ using different techniques. It was reported that both the type and concentration of the dopant have an influence in changing both properties and structure of the polymer.

Electron spin resonance (ESR) spectroscopy is one of the most widely used and productive physical methods in structural and magnetic studies of polymers, which contain transition metal complexes.[9] The magnetic properties of PVA films filled with some 3d-transition metal ions (Mn^{2+}, Cu^{2+}, and VO^{2+}) were reported.[10–12] The structural, optical, thermal, electrical, and magnetic properties of polymers can be suitably modified by the addition of some metal compounds depending on their reactivity with the host matrix. In the present work, we study the structural, optical, and magnetic properties of PVA films filled with various concentrations of $CoBr_2$ using different spectroscopic techniques.

EXPERIMENTAL

Samples preparation

The PVA used in this work were obtained in pellet form from Merck, Germany had a molecular weight 14,000. PVA films with different amounts of $CoBr_2$ dopant were prepared by solvent casting technique.

Correspondence to: I. S. Elashmawi (islam_shukri2000@yahoo.com).

A known quantity of PVA pellets was added to doubly distilled water and kept for 48 h while stirring the solution at 70°C for complete dissolution. Required quantity of $CoBr_2$ was also dissolved in doubly distilled water and added to the polymeric solution with continuous stirring. The solution was poured onto cleaned the Petri dishes and dried in an oven at 50°C. After drying, the films were peeled from the Petri dishes and kept in vacuum desiccators until use. The thickness of the obtained films was in the range of 100–120 μm. PVA films doped with $CoBr_2$ mass fractions of 0, 2.5, 5, 7.5, 10, 12.5, 15, 17.5, and 20 weight percentage (wt %) were prepared by using the relation:

$$\text{wt\%} = \frac{w_d}{w_p + w_d} \times 100 \quad (1)$$

where w_d and w_p are the weight of dopant and polymer, respectively.

Physical measurements

The FTIR measurements were carried out using the single beam Fourier transform infrared spectrophotometer (FTIR-430, Jascow, Japan). The FTIR spectra of the samples were obtained in the spectral range of 4000–600 cm^{-1} with scanning speed of 2 mm/s. Ultra violet and Visible (UV/VIS) absorption spectra were measured in the wavelength region of 220–800 nm using a Spectrophotometer (Perkin Elmer UV/VIS).

The X–ray diffraction (XRD) scans were obtained using DIANO corporation equipped with CuK_α radiation ($\lambda = 1.540$ Å, the tube operated at 20 kV, the Bragg angle (2θ) in the range of 5°–60°, step size = 0.1, and step time 1 s). The differential scanning calorimetry (DSC) for the prepared films was carried out using an equipment type (GDTD16-Setaram) with measuring temperature range from room temperature to 300°C and heating rate 10°C/min. Electron spin resonance (ESR) spectra were recorded on JEOL spectrometer type (JES-FE2XG).

RESULTS AND DISCUSSION

FTIR analysis

Figure 1 shows FTIR absorption spectra of PVA filled with different concentrations of $CoBr_2$ recorded at room temperature in the region 4000–600 cm^{-1}. The spectra exhibit bands characteristic of stretching and bending vibrations of O—H, C—H, C=C, and C—O groups.[13–15] From FTIR spectra, the band at 3484 cm^{-1} is assigned to O—H stretching vibration of hydroxyl groups of PVA. The band corresponding to CH_2 asymmetric stretching vibration occurs at 2938 cm^{-1} and C—H symmetric stretching

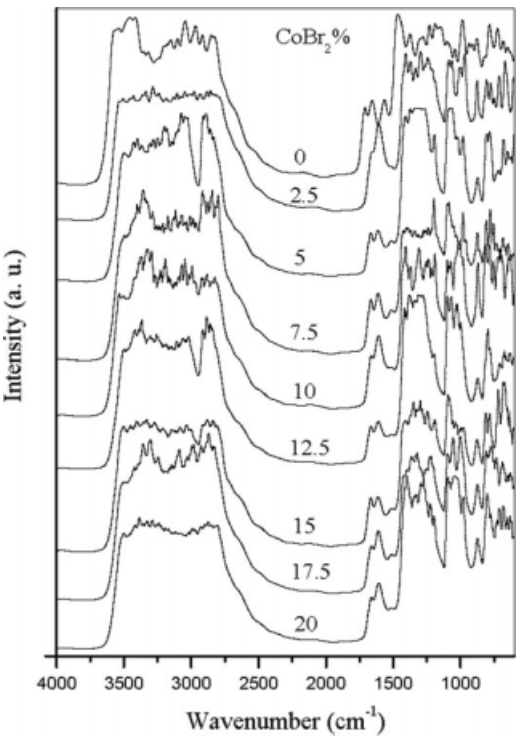

Figure 1 FTIR spectra of PVA films doped with $CoBr_2$.

vibration at 2853 cm^{-1}. The absorption band at 1733 cm^{-1} is generally ascribed to C=O stretching. This also provides the evidence that PVA used in this study still has some acetyl groups, that is, it is only partially hydrolyzed. The weak band at 1640 cm^{-1} corresponds to C=C. It is remarkable that the present double bonds segments are considered as suitable sites for polarons and/or bipolarons.[13] The band at 760 cm^{-1} which is assigned to C—Br stretching and C—H bending exhibits changes in its intensity behavior with wt %. This band is sensitive to head to head defects. The band at 1089 cm^{-1} corresponds to C—O stretching of acetyl groups present on the PVA back bone.[10,14] The corresponding bending, wagging of CH_2 vibrations at 3592 cm^{-1}, respectively, and C—H vibration wagging mode at 1247 cm^{-1}.

In the case of $CoBr_2$ doped PVA films, the FTIR spectra shows shifts in the corresponding bands with a change in intensities. This indicates the considerable interaction between PVA and $CoBr_2$. From the figure, it is clear that the stretching frequencies of acetyl C=O of PVA shifts from 1658 cm^{-1} to 1650 cm^{-1}. The stretching frequency of C=C was shifted from 1733 to 1729 cm^{-1}. The shift in bending of CH_2 vibrations are from 1448 to 1434 cm^{-1} indicates the chemical interactions of Co^{+2} ions with PVA matrix.

The PVA structural deformations due to the filling by $CoBr_2$ can be understood by plotting the intensity of the absorption peak at 3040 cm^{-1} due to radical R—HC=CH_2 as a function of the weight (w) of

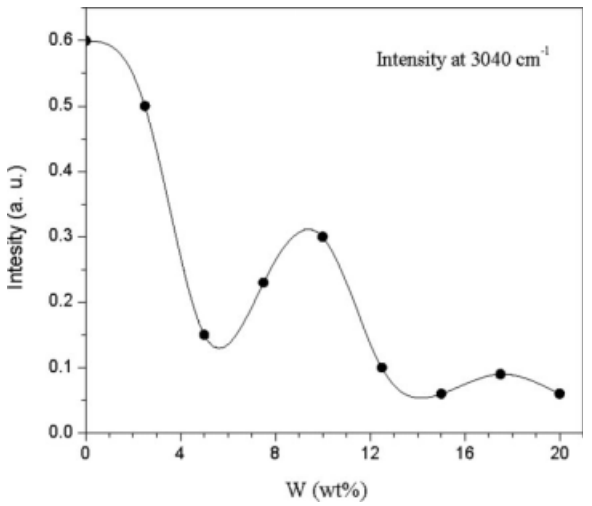

Figure 2 The FL dependence of the intensity at 3040 cm^{-1}.

$CoBr_2$ as shown in Figure 2. This peak will be correlated with the magnetic properties.[15]

UV–visible studies

Figure 3 shows the ultraviolet optical absorption spectra of pure PVA filled with different concentrations of $CoBr_2$ recorded at room temperature in the range of wavelength from 200–2000 nm. The absorption bands at 280 nm is assigned to $\pi \rightarrow \pi^*$ transition which comes from unsaturated (double) bonds, C=O and/or C=C mainly in the tail to head of PVA.[16] The sharp absorption edge around 244 nm in pure PVA indicates the semi-crystalline nature of PVA. A shift in band edges towards the higher wavelengths with different absorption intensity for the doped PVA was observed. These shifts in the bands indicate the formation of inter/intramolecular hydrogen bonding mainly between Co^{+2} with OH groups that are in consistence with FTIR results. Also, the shift in absorption edge in the doped PVA films reflects the variation in the energy band gap, which arises from the variation in crystallinity with in PVA polymeric matrix. The optical spectra of the filled films contain weak and broad visible bands at 500 nm was attributed to the transition $^4T_{1g}$ (F) $\rightarrow$ $^4T_{1g}$ (p), for the octahedral Co^{+2} structure.[17] The optical energy gap for direct transition can be determined by using the relation:

$$E_g = h\nu - (\alpha h\nu/B)^{1/2} \quad (2)$$

where h is plank's constant, ν is the photon frequency, B is a constant, and α is the absorption coefficient, which can determined as a function of photon frequency using the equation:

$$\alpha = \frac{A}{d} \times 2.303 \quad (3)$$

where A is the absorbance and d is the thickness of the sample. The plot of $(\alpha h\nu)^{1/2}$ verses the photon energy $h\nu$ at room temperature shows a linear behavior which are presented in Figures 4 and 5. Each linear portion indicates an optical band gap E_g which can be considered as an evidence for direct allowed transition. The obtained values of the band

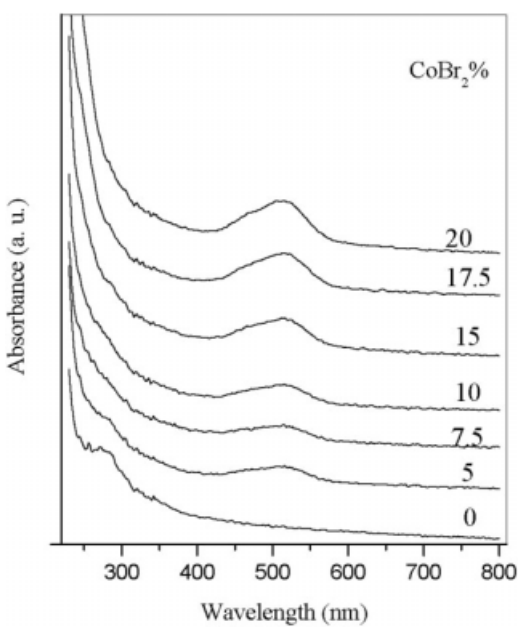

Figure 3 UV–vis absorption spectra of PVA films doped with $CoBr_2$.

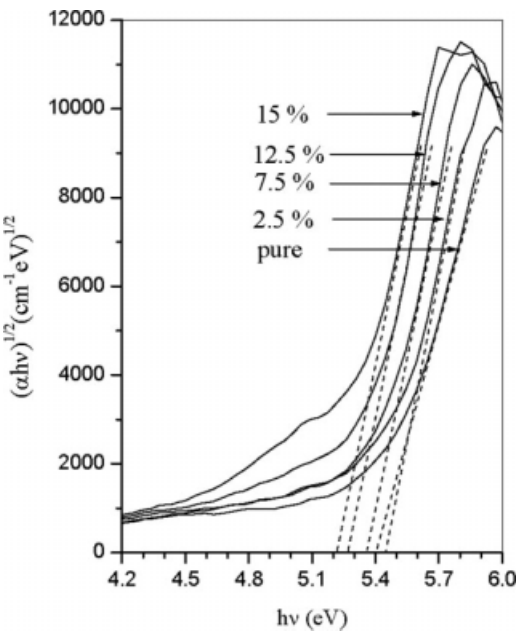

Figure 4 Optical energy gap of PVA films doped with 2.5, 7.5, 12.5, and 17.5 wt % of $CoBr_2$.

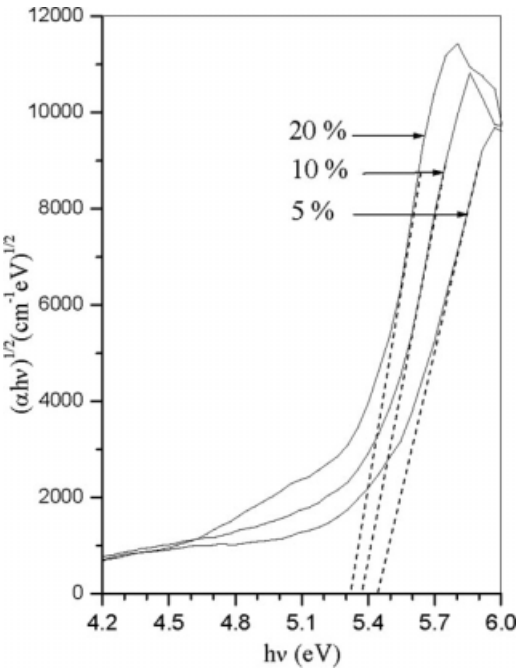

Figure 5 Optical energy gap of PVA films doped with 0, 5, and 10 wt % of $CoBr_2$.

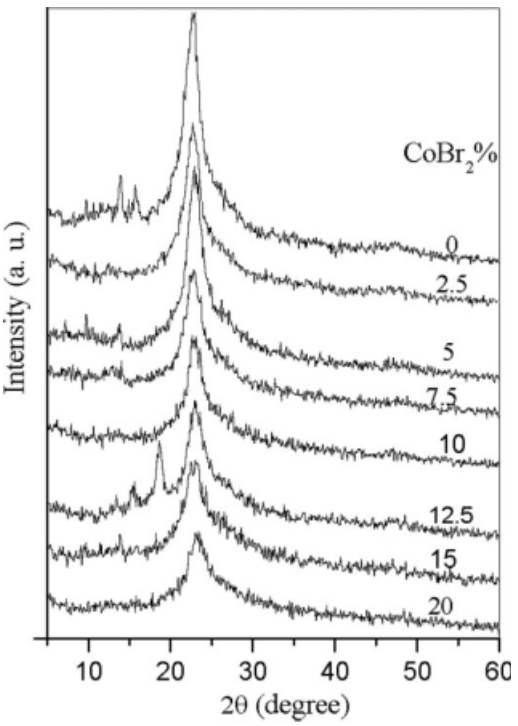

Figure 6 X-ray diffraction scans pure PVA films doped with $CoBr_2$.

gap E_g (as shown in Table I) decreases from 5.45 eV to 5.21 eV with increasing different concentrations of $CoBr_2$. The existence and variation of optical energy gap E_g may be explained by considering the occurrence of local cross linking within the amorphous phase of PVA.

X-ray diffraction studies

Figure 6 represents the X-ray diffraction scans of PVA films. The figure shows relatively sharp peaks at $2\theta \sim 14^\circ$, $2\theta \sim 16^\circ$, and a broad peak centered at $2\theta \sim 22^\circ$ ($d = 3.554$ Å) reveal the semicrystalline nature of the polymer PVA containing crystalline and amorphous structure.[18] This peak corresponds to (110) reflection. It is well known that the crystalline PVA has diffraction peak angle at $2\theta \cong 22^\circ$. It was noted that the decrease in the relative intensity of this diffraction peak with increase of $CoBr_2$ concentration, this reveals decreases the degree of crystallinity. Moreover, the degradation of PVA led to the formation of new carbonyl bands of several carbon-carbon bands, which can be observed in the FTIR spectrum. The decrease of the PVA crystalline diffraction peak was attributed to the interaction between PVA and the filler. PVA that was usually crystalline resulted from the string intermolecular interaction among PVA chains through intermolecular hydrogen bonding. The intensity of the diffraction and also the size of the crystals of PVA are determined by the number of PVA chains packing together. The complexation of PVA chains with $CoBr_2$ would lead to a decrease in the intermolecular interaction between the PVA chains and the degree of crystallinity.[19] This confirms the presence of $CoBr_2$ crystallites within the polymeric matrix.

TABLE I
Optical Energy Gap, Melting and Decomposition Temperatures of the Pure PVA and PVA with Different Concentrations of $CoBr_2$

$CoBr_2$ (wt %)	E_g (eV)	T_m (°C)	T_d (°C)
0	5.45	207.21	267.55
2.5	5.40	205.38	262.60
5.0	5.38	204.24	257.07
7.5	5.36	200.43	250.35
10	5.34	199.02	224.26
12.5	5.29	198.26	239.76
15	5.26	194.06	235.33
20	5.21	190.76	230.52

Differential scanning calorimetry

The thermal behavior of the pure PVA and the PVA/$CoBr_2$ composite films was studied by DSC to estimate how the thermal transitions of the prepared films were affected by the different concentrations of $CoBr_2$ from room temperature to 300°C. DSC thermograms is shown in Figure 7. As can be seen, the thermogram is characterized by two endothermic peaks for pure PVA and PVA/$CoBr_2$ composite films. The endothermic peak (for pure PVA) at about

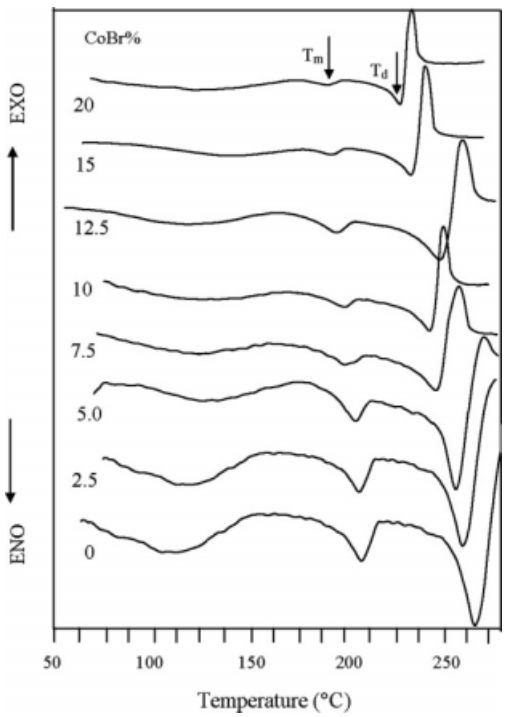

Figure 7 DSC thermograms of PVA with different concentrations of $CoBr_2$.

207.21°C was assigned to the melting temperature[20,21] T_m, which indicates the semicrystalline nature of the PVA. A sharp endothermic peak (T_d) is noticed at $T_d \approx 267.55$°C due to the polymer decomposition.[20] Table I shows the variation of T_m and T_d with different concentrations of $CoBr_2$. From this table, the decrease in T_m might be due to the effect of the doping of $CoBr_2$ on the orientation of the degree of crystallinity and microstructure of the samples. Similar behavior is also in the XRD study. This implies that the crystalline phase decreases with increasing the different concentrations of $CoBr_2$. Also, it is clear that the magnitude of T_d of the pure PVA films was greater than those of PVA/$CoBr_2$ composite films. Apparently, the addition of $CoBr_2$ to PVA films can reduce the thermal stability.

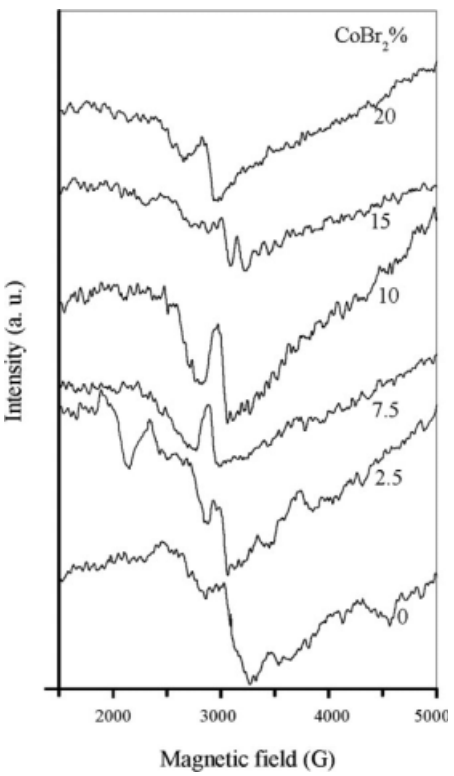

Figure 8 ESR spectra of PVA films doped with 0, 2.5, 7.5, 10, 15, and 20 wt % of $CoBr_2$.

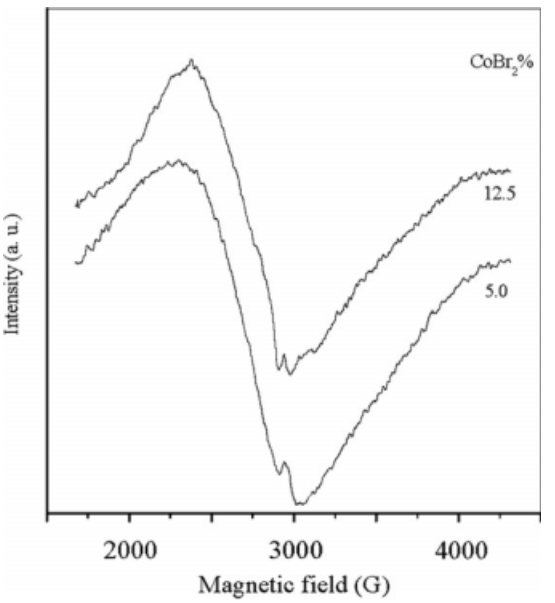

Figure 9 ESR spectra of PVA films doped with 5 and 12.5 wt % of $CoBr_2$.

Electron spin resonance analysis

The ESR spectrum of PVA-filled and unfilled $CoBr_2$ is shown in Figures 8 and 9. Pure PVA is

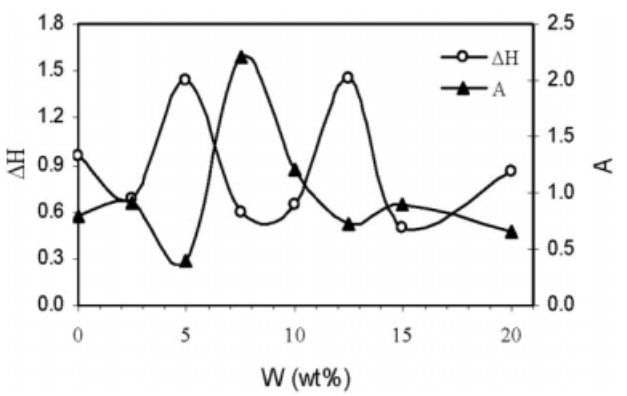

Figure 10 The FL dependence on ΔH and asymmetry factor.

characterized by broad signals due to polymeric matrix and hyperfine lines due to free radicals. The obtained spectra may arise from residual free carriers and/or neutral defects in the PVA chain structure. The present signals are located around g-factor ($g \sim 2.022$) coupled by strong dipolar and super exchange interactions. In some of such structural defects, the unpaired electron results from a domain wall in the bond alternation resulting in a neutral π-electron free radical. This unpaired electron would be delocalized over several carbon atoms. Such defects could arise principally in the isomerization process. On the other hand, the ESR may arise from σ-electron radicals, exhibiting g-factor $< g_e$ (the free electron g factor). These electrons are expected to be localized in an SP^2 or SP^3 orbital, so the hyperfine splitting from adjacent ^1H or ^{13}C nuclei would be easily distinguished if trans-defects occurred in the π-system.

The filling level (FL) dependence of the filler local structure can be clarified more explicitly with the aid of the peak-to-peak separation of ΔH of the main ESR Lorentzian signal and the asymmetry factor (A) which is the ratio between the two halves of this signal. The obtained values of ΔH and A are plotted, as functions of wt %, as shown in Figure 10. It is clear that the behavior of ΔH is the mirror image to the behavior of asymmetry factor. A maximum value of ΔH, which means the sharpest ESR signal, is noticed at wt = 12.5%. This can be attributed to the mesomorphous phase, found at this filling level.

CONCLUSIONS

Spectroscopic, structural and magnetic properties of PVA filled with $CoBr_2$ were investigated by FTIR, UV–visible, X-ray, and ESR measurements and compared those of PVA alone. The FTIR spectrum shows that the filler interacts with the OH groups of PVA. The observed weak and strong bands in the spectrum indicates the presence of bending and stretching vibrational modes of C—H, C—O, O—H, C=O, and C=C groups. UV–visible optical also confirm the complex formation and its effect on the microstructure. This change is due to complex formation which can be reflected in the form of variation in the optical energy gap. X-ray analysis shows that the change of the structure due to the interaction of dopant with the polymer, which decrease in the degree of crystallinity. The DSC thermograms depicts that the addition of $CoBr_2$ decreased the melting and decomposition temperatures. This also suggests that the interaction of $CoBr_2$ and PVA molecule changes the degree of crystallinity, which supports the X-ray results.

References

1. Lopez, D.; Cendoyo., I.; Torres, F.; Teijad, J.; Mijango, C. J Appl Polym Sci 2001, 82, 3215.
2. Yamaura, K.; Kuramuki, N.; Suzuki, M.; Tanigami, T.; Matsuzawa, S. J Appl Polym Sci 1990, 41, 2409.
3. Zidan, H. M. J Appl Polym Sci 2003, 88, 104.
4. Tawansi, A.; El-Khodary, A.; Abdelnaby, M. M. Curr Appl Phys 2005, 5, 572.
5. Selim, M. S.; Seoudi, R.; Shabaka, A. A. Mater Lett 2005, 59, 2650.
6. Beck, A.; Horváth, A.; Stefler, G. Y.; Katona, R.; Geszti, O.; Tolnai, G.y; Liotta, L. F.; Guczi, L. Catal Today 2008, 139, 180.
7. Bhajantri, R. F.; Ravindrachary, V.; Harisha, A.; Crasta, V.; Nayak, S. P.; Poojary, B. Polymer 2006, 47, 3591.
8. El-Khodary, A.; Oraby, A. H.; Abdelnaby, M. M. J Magn Magn Mater 2008, 320, 1739.
9. Ranby, B.; Rabek, J. F. ESR Spectroscopy in Polymer Research; Springer: New York, 1977.
10. Kumar, G. N.; Rao, J. L.; Gopal, N. O.; Narasimhulu, K. V.; Chakradhar, R. P. S.; Rajulu, A. V. Polymer 2004, 45, 5407.
11. Kumar, M.; Dhobale, A. R.; Kadam, R. M.; Sastry, M. D. J Phys 1994, 52, 647.
12. Kumar, M.; Dhobale, A. R.; Kumar, M.; Sastry, M. D. J Polym Sci Part B: Polym Phys 1997, 35, 187.
13. Omkarama, I.; Chakradhar, R. P. S.; Rao, J. L. Phys B 2007, 388, 318.
14. Sun, Z.; Sun, Y.; Yang, X.; Zheng, Z. Surf Coat Technol 1996, 79, 108.
15. Hirankumar, G.; Selvasekarapandian, S.; Kuwata, N.; Kawamura, J.; Hattori, T. J Power Sources 2005, 144, 262.
16. Allanand, J. R.; Bonner, J. G. Eur Polym J 1986, 22, 973.
17. Davis, E. A.; Mott, N. F. Philos Mag 1970, 22, 903.
18. Hong, P. D.; Chen, J. H.; Wu, H. L. J Appl Polym Sci 1998, 69, 2477.
19. Qian, X. F.; Yin, J.; Yang, Y. F.; Lu, Q. H.; Zhu, Z. K.; Lu, J. J Appl Polym Sci 2001, 82, 2744.
20. Yua, Y.; Lina, C.; Yeha, J.; Lin, W. Polymer 2003, 44, 3553.
21. Bin, Y.; Mine, M.; Koganemaru, A.; Jiang, X.; Matsuo, M. Polymer 2006, 47, 1308.